

Evaluation of Mechanical Properties and Pyrolysis Products of Carbon Fibers Recycled by Microwave Pyrolysis

Yiyao Ren, Lei Xu,* Xiaobiao Shang, Zhigang Shen,* Rongzheng Fu, Wei Li, and Lirong Guo

Cite This: *ACS Omega* 2022, 7, 13529–13537

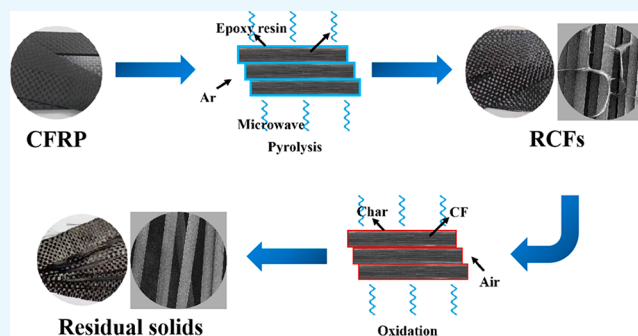
Read Online

ACCESS |

Metrics & More

Article Recommendations

ABSTRACT: Disposal of the waste from carbon fiber reinforced polymers (CFRPs) has become an urgent problem due to the increasing application of CFRPs in many industries. A novel method for the rapid recovery of carbon fibers by a microwave pyrolysis and oxidation process was proposed in this study. The resin matrix was rapidly pyrolyzed by heating CFRPs directly with microwave radiation, and then the residual carbon and organic matter on the surface of carbon fibers were removed by oxidation to obtain recycled carbon fibers (RCFs). The recovery rate of recycled carbon fibers was measured, and their mechanical properties were evaluated by tensile strength and tensile modulus tests. The results showed that, after microwave pyrolysis at 500 °C for 15 min and oxidation at 550 °C for 30 min, the maximum tensile strength of RCFs was 3042.90 MPa (about 99.42% of that of virgin carbon fibers), the tensile modulus was 239.39 GPa, and the recovery rate was about 96.5%. The microstructure and chemical composition of RCFs were characterized by scanning electron microscopy, X-ray diffraction, Raman spectroscopy, Fourier transform infrared spectroscopy, and X-ray photoelectron spectroscopy, and the components of the pyrolysis byproducts were detected by gas chromatography–mass spectrometry. These results indicate that this method is suitable for the effective recovery of high-quality carbon fibers from CFRPs.



1. INTRODUCTION

Carbon fiber reinforced polymers (CFRPs) have higher specific strength than metal materials, as well as excellent properties such as high temperature resistance, corrosion resistance, and impact resistance.^{1,2} These characteristics make CFRPs powerful substitutes for traditional metal materials in the automobile, vessel, aviation, and aerospace fields.^{3–5} The annual consumption of carbon fibers (CFs) is about 100000 tons, 15.4% of which is used in the aerospace field and 11.7% in the automobile industry, and the annual market of CFs is growing by more than 11%.⁶ In recent years, the biggest challenge facing the automobile and aircraft industry has been to find ways to save fuel and reduce weight to reduce carbon dioxide emissions. CFRPs have been widely used in the automobile industry as an effective means to realize lightweight vehicles.⁷ By 2022, the demand for CFs is expected to reach 117000 tons.^{2,7} The increasing demand of CFs will result in more and more CFRP waste, making the disposal of CFRPs an urgent problem.

At present, most CFRP wastes are disposed of by landfill.⁸ Epoxy resin is widely used in CFRPs because of its low viscosity, good compatibility with the fiber surface, heat resistance, and excellent mechanical properties. However, after being disposed of as industrial waste in landfills, CFRPs have caused tremendous resource waste and serious environmental

problems such as landscape destruction, soil pollution, and water pollution.^{9–11} After CFRPs are disposed of in a landfill, the partial degradation of the resin will produce toxic substances remaining on the land, causing soil pollution. In addition, toxic substances will cause water pollution when they are transferred into the water.^{2,6} Consequently, most developed countries have started to legally prohibit the landfill disposal of CFRPs. In addition, the use of CFRPs as vehicle materials has greatly increased the necessity of developing a recycling technology.¹² Therefore, it is imperative to recycle CFs.

Generally, the main recycling methods of CFs include mechanical,^{13–15} chemical,^{16–19} and thermal methods.^{20–22} In the mechanical method, CFRP waste is crushed into particles or milled into powder, which can be directly used as a filler. Only short CFs can be obtained by the mechanical method, and their mechanical properties are severely damaged after

Received: November 24, 2021

Accepted: April 4, 2022

Published: April 15, 2022



Scheme 1. Cyclic Utilization Route of Carbon Fibers

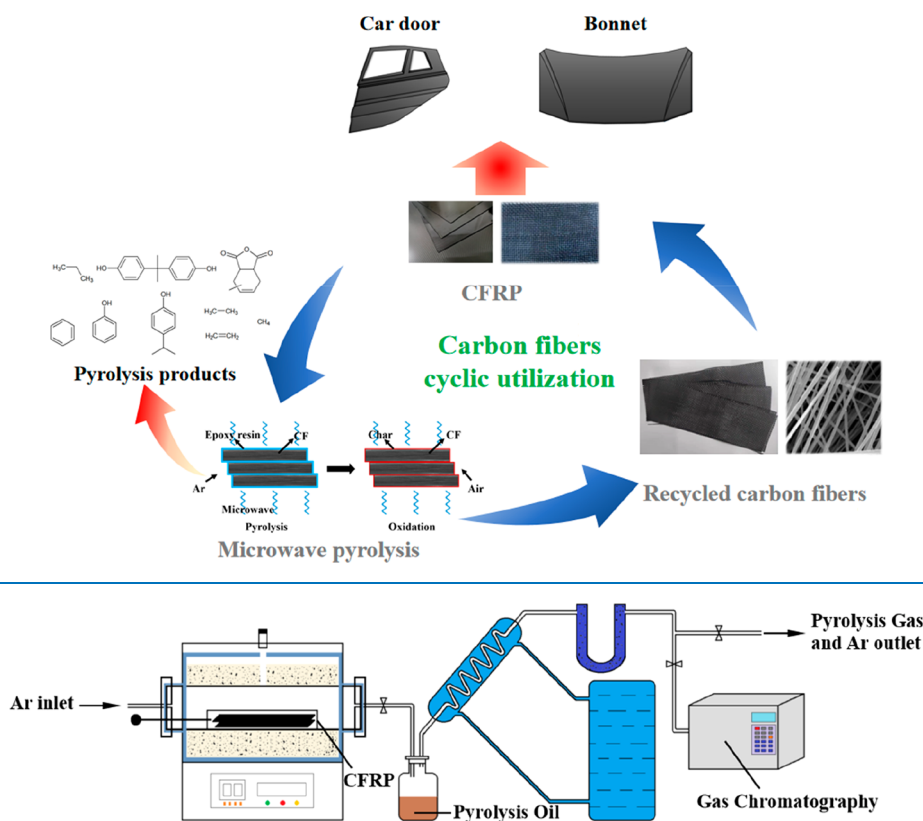


Figure 1. Schematic diagram of microwave pyrolysis.

grinding and shearing.¹² In the chemical method, the cross-linked bonds in the resin are broken by solvent and heat and the resin is decomposed into low-molecular-weight polymers or small organic molecules and dissolved in the solvent, thereby separating CFs from the resin matrix. CFs recycled by chemical method can retain a tensile strength of 80% and up to 99% under extreme conditions. However, this is not an appropriate recovery method because it involves high cost and produces harmful gases,²¹ such as nitrogen oxides, sulfides, and volatile organic solvents. In the pyrolysis method, the resin in the composite is decomposed into small organic molecules at high temperature to recover CFs. At present, pyrolysis is used in most commercial-scale CF recycling operations in the world.² When CFs are recycled by pyrolysis, the tensile strength of the recycled carbon fibers (RCFs) can be maintained at 50–85%,⁷ and long CFs can be obtained. More importantly, recycling CFs by pyrolysis can save energy and reduce the environmental impact. The production of virgin carbon fibers (VCFs) requires 198–595 MJ/kg of energy consumption and emits 30–80 kg of CO₂,^{23–25} while RCFs consume only 30 MJ/kg and emit less CO₂.²⁴

Microwave radiation has been used as a heat source in the pyrolysis of composites.⁶ Microwave heating has the characteristics of internal, rapid, and selective heating, which has broad development potential in the preparation, sintering, and recycling of materials.²⁶ The materials recovered by microwave technology mainly include metals,²⁷ lithium-ion batteries,²⁸ CFRPs, spent carbon cathodes,²⁹ sewage,³⁰ and circuit boards.³¹ Lester³² of the University of Nottingham and others studied the feasibility of recycling the CF/epoxy resin

composite material recovery by microwave pyrolysis and proved that microwave heating could effectively recycle CFs.

Microwave-assisted pyrolysis was used for recycling CFs in this study, which was different from the traditional pyrolysis method. Scheme 1 shows the cyclic utilization route of CFs. First, CFs are recycled from CFRP waste by microwave pyrolysis. Then the obtained RCFs are converted into thermoplastic or thermosetting composites to realize the cyclic utilization of CFs in the automobile, sports, construction, aerospace, and electric power fields. In this study, the technical advantages of microwave heating were combined with the technical characteristics of recycling CFs from CFRP by the pyrolysis method. The epoxy resin in CFRPs was decomposed by direct microwave heating, and then the pyrolyzed carbon and residual organic matter on the CF surface were removed by oxidation. The surface morphology, recovery rate, mechanical properties, chemical structure of RCFs and the components of the pyrolysis byproducts were characterized to investigate the effects of different reaction conditions on the recycling of CFs.

2. EXPERIMENTAL SECTION

2.1. Materials. CFRP sheets with a size of 100 × 20 × 1 mm were provided by Gongyi Fanruiyihui Composites Co., Ltd., Henan Province, China. The VCFs were produced by Formosa Plastics Group in Taiwan. CFRP was prepared with epoxy resin (E51) as s matrix, carbon fiber cloth (TC33-3K) as s reinforcement, methyl tetrahydrophthalic anhydride (Meth-PA) as s curing agent, and tris(dimethylaminomethyl)phenol (DMP-30) as an accelerator. The carbon fiber cloth was plain woven, and the above/below pattern of the wire rope was

woven to provide a highly stable and compact structure. Each CFRP sheet contains six layers of carbon fiber cloth. CFs in CFRP have a mass fraction of about 76 wt % and a volume fraction of about 68 vol %.

2.2. Experimental Procedure. The pyrolysis and oxidation of CFRPs were studied in a microwave tube furnace and a traditional tube furnace respectively. The schematic diagram of the experimental device is shown in Figure 1. The microwave frequency was 2.45 ± 0.05 GHz, and the microwave power was 0–1000 W. The microwave tube furnace was connected to an argon gas cylinder, a pyrolysis oil collection bottle, a condenser tube, a drying tube, and an exhaust pipe. Before the reaction, argon gas was first introduced into the furnace, and then the air was exhausted for several minutes. This process was repeated three times to ensure the complete removal of air. After the argon gas was stably introduced into the microwave tube furnace with a flow rate of 50 mL/min, microwave radiation was applied, and the CFs in CFRPs were directly heated by microwave radiation, so that the resin could be pyrolyzed quickly. Part of the pyrolysis gas was condensed to form an oil, and the noncondensable part and argon gas were collected after drying. After the pyrolysis experiment, the solids were cooled to room temperature, and the residual solids were taken out and put into a traditional tube furnace. After introduction air, the pyrolytic carbon and residual organic matter on the CF surface were oxidized for a period of time, and finally the RCFs were obtained. The experimental scheme and sample code are presented in Table 1.

Table 1. Experimental Scheme and Sample Code

experiment (sample code)	microwave pyrolysis		experiment (sample code)	thermal oxidation	
	temp (°C)	time (min)		temp (°C)	time (min)
P400T15	400	15	DS00T40	500	40
			DS00T50	500	50
P500T15	500	15	D550T30	550	30
			D550T40	550	40

2.3. Characterization Methods. Thermogravimetric analysis (TGA) data of CFRP pyrolysis were collected with a DSC/DTA-TG analyzer (STA 449 F3 Jupiter, Netzsch, Germany). The CFRP (10 mg) sample was heated from 30 to 1000 °C at an increment of 15 °C/min under an argon atmosphere with a flow rate of 20 mL/min. The residual solids (10 mg) were heated from 30 to 1000 °C in an air atmosphere with a flow rate of 20 mL/min at an increment of 15 °C/min. The surface morphology of RCFs was observed by a scanning electron microscope (SEM, VEGA3 SBH, TESCAN, Czech). The mechanical properties of RCFs were tested by an automatic single-fiber universal tester (Robot 2, Textechno, Germany). The structure of RCFs was detected by X-ray diffraction (XRD, Rigaku Ultima IV, Japan) with a scanning speed of 5°/min in the scanning range of 10–80°. The absorption spectra of the functional groups in RCFs were characterized by Fourier transform infrared spectroscopy (FT-IR, Nicolet IS 50, Thermo Nicolet, USA) with a spectral resolution of 4 cm⁻¹ in the range of 1000–3000 cm⁻¹. Raman spectra of RCFs were obtained with a laser wavelength of 532 nm and a scanning wavenumber ranging from 500 to 2300 cm⁻¹ (LabRAM HR Evolution, Horiba Scientific, France). The

surface elements and groups of RCFs were analyzed by X-ray photoelectron spectroscopy (XPS, K-Alpha+, Thermo Fisher Scientific, USA). The compositions of the pyrolysis oil and gas were detected by gas chromatography–mass spectrometry (GC-MS, Thermo Finnigan Trace DSQ, USA), in which the pyrolysis oil and gas were tested by a headspace method and a direct injection method, respectively.

3. RESULTS AND DISCUSSION

3.1. Analysis of Pyrolysis Process. To study the pyrolysis behavior of CFRPs and the oxidation behavior of residual solids, thermogravimetric analyses were carried out under atmospheres of argon and oxygen, respectively. As can be seen from the TG curve in Figure 2a, the relative mass of residual solids after pyrolysis is about 77%, which is slightly higher than the mass fraction of CFs in the CFRPs provided by the manufacturer. This is due to the formation of pyrolytic carbon during pyrolysis.¹⁹ The epoxy resin in the CFRPs began to pyrolyze at about 300 °C, and the pyrolysis was finished at about 600 °C. Therefore, a pyrolysis temperature of CFRPs at 400–800 °C is more suitable. As can be seen from the DTG curve in Figure 2b, the residual solids are slowly oxidized in the range of 350–600 °C, and the oxidation rate increases sharply after exceeding 600 °C due to the oxidization of CFs, which is not conducive to the control of the oxidation degree. On consideration of the performance, recovery rate, and processing efficiency of RCFs, the suitable oxidation temperature in the experimental research process was set in the range of 500–600 °C.

To further study the effect of microwave radiation on the pyrolysis process of CFRPs, the electromagnetic field and temperature distribution during the microwave heating of CFRP were simulated with COMSOL software. The cavity of the microwave tube furnace and CFRP sheet were designed on the basis of the actual object. As shown in Figures 2c,d, the dimensions of the furnace cavity and CFRP sheet are 31 × 28 × 26 and 10 × 2 × 0.1 cm, respectively. Figure 2e shows the distribution of the electromagnetic field in the furnace cavity, which is not symmetrical because the microwave generator is in the upper left part instead of the center of the microwave tube furnace. Figure 2f,g gives the distributions of the electromagnetic and temperature fields on the surface of CFRPs, respectively, indicating that the distribution of temperature is directly related to the distribution of electromagnetic field and that the stronger the electromagnetic field, the higher the temperature. Figure 2h compares the actual heating curves and the simulated heating curve. The simulated power was 500 W, and the actual powers were 400 and 500 W. It shows that the simulated heating curve has a high degree of fitting with the actual curve, suggesting that the simulation results will be consistent with the experimental results.

3.2. Mechanical Properties of RCFs. The macroscopic morphologies of CFRP, residual solids, and RCFs are shown in Figure 3. Figure 3a indicates that CFs are coated with epoxy resin and tightly bonded together in CFRPs. Figure 3b shows the residual solids obtained after pyrolysis of CFRPs, which have a flaky structure and easily delaminate, but there are no filamentary products. RCFs shown in Figure 3c cannot be obtained directly, but they are obtained from oxidizing the residual solids, which are filamentous products that can be easily dispersed.

The microscopic morphology of VCFs is shown in Figure 3d, and the fiber surface is smooth and defect-free with a

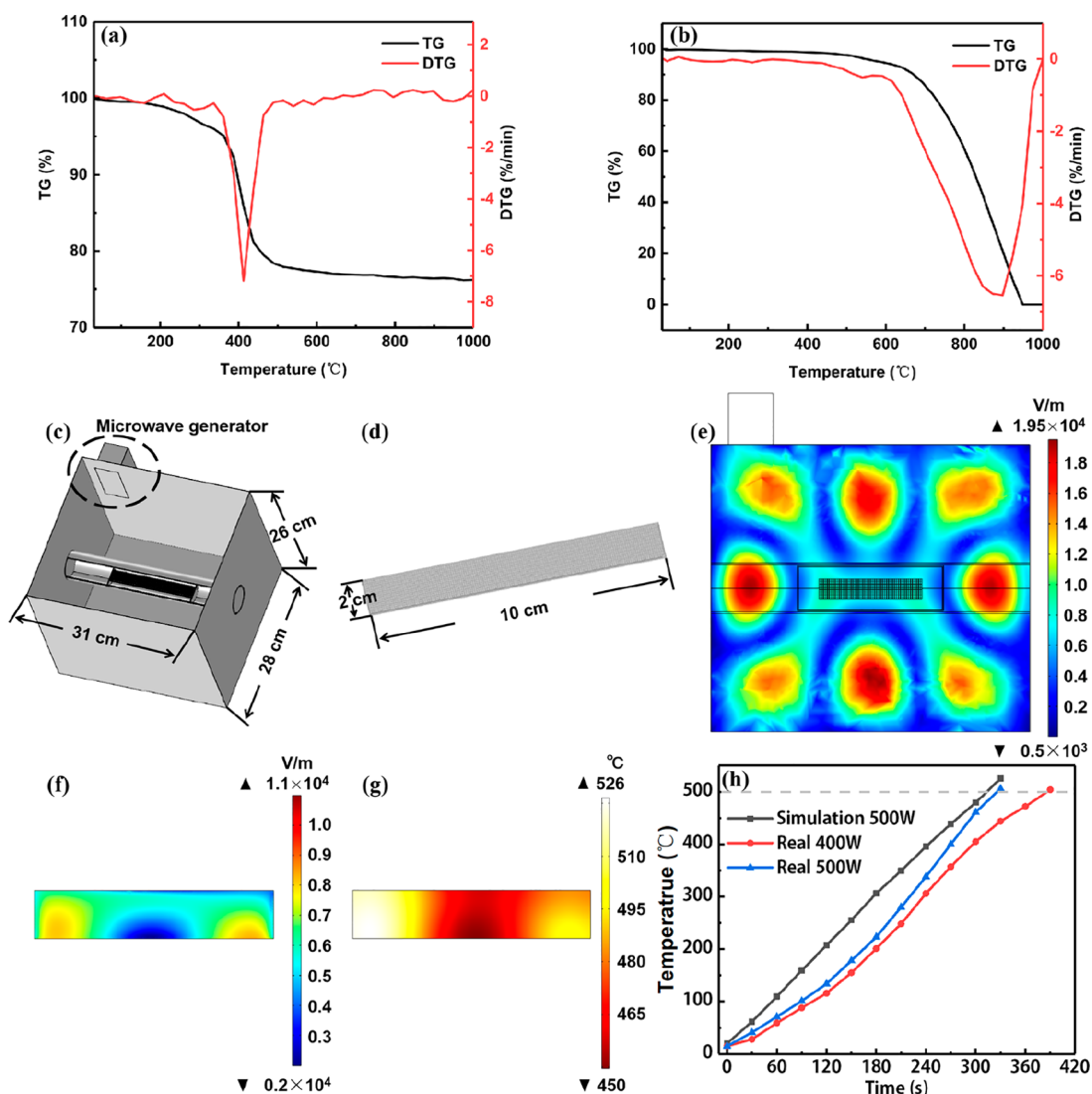


Figure 2. Thermogravimetric analysis of (a) CFRP under an argon atmosphere and (b) residual solids in an air atmosphere and simulation results of (c) a model of the furnace cavity, (d) a model of CFRPs, (e) electromagnetic field distribution in the furnace cavity, (f) electromagnetic field distribution on CFRPs, (g) temperature field distribution on CFRPs, and (h) heating curves.

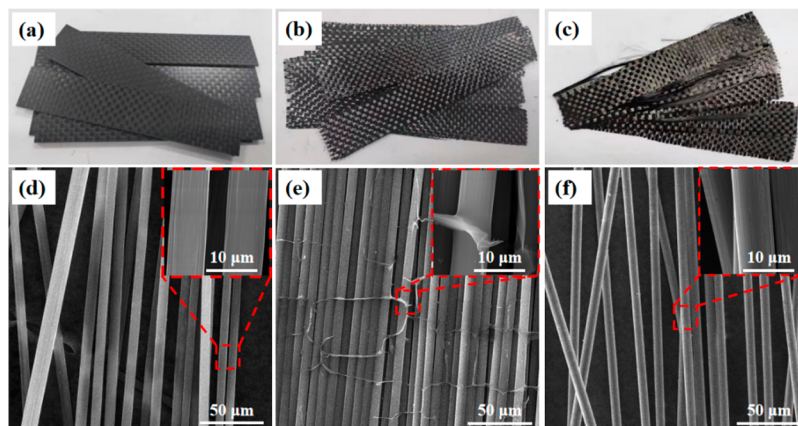


Figure 3. Pictures of (a) CFRP, (b) P500T15, and (c) P500T15D550T30 and SEM images of (d) VCFs, (e) P500T15, and (f) P500T15D550T30.

grooved structure. The microscopic morphology of residual solids shown in Figure 3e indicates that some carbon residue is deposited on the surface of CFs after pyrolysis, which makes it

difficult to separate a single carbon fiber. Laura et al.³³ also observed that CFs after pyrolysis were covered by pyrolytic carbon, which was caused by decomposition of the resin.

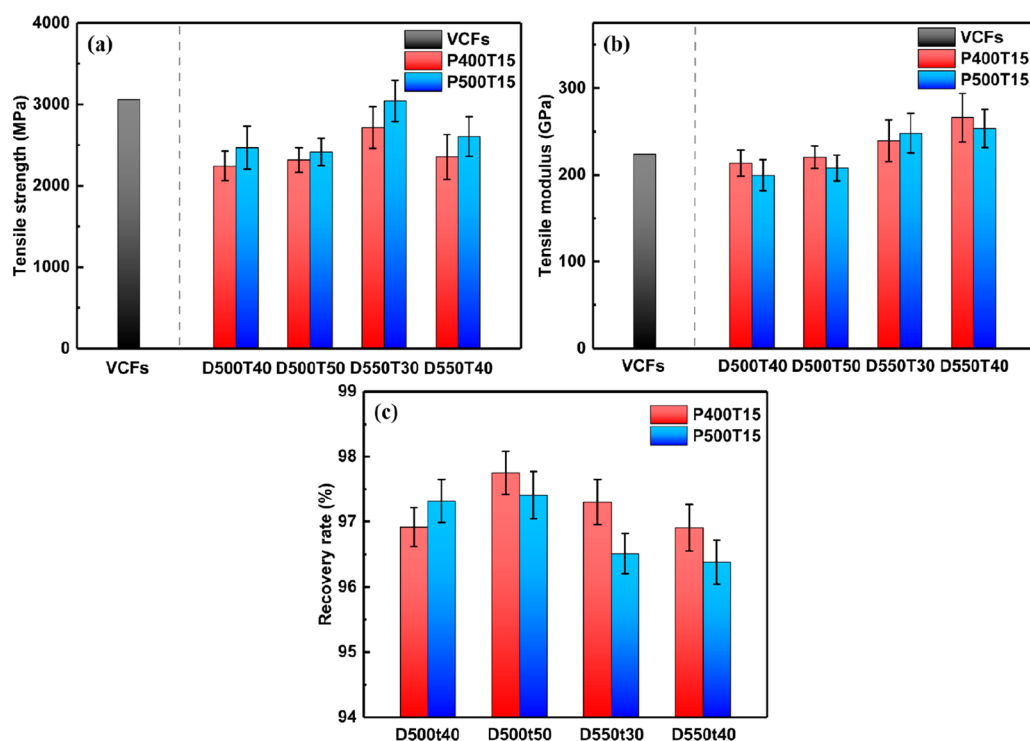


Figure 4. Mechanical properties and recovery rate of RCFs: (a) tensile strength; (b) tensile modulus; (c) recovery rate.

Figure 3f shows the microscopic morphology of RCFs obtained by oxidation, indicating that after the residual solids are oxidized at 550 °C for 30 min the surface of RCFs is smooth and clean, without carbon deposition and resin residue, and the grooved structures are retained.

By measurement of the mechanical properties and recovery rate of RCFs, the effects of different recycling conditions were evaluated. Figure 4a shows the tensile strength of RCFs. With an increase in oxidation temperature and oxidation time, the tensile strength of RCFs first increased and then decreased. Under the condition of high oxidation temperature and long oxidation time, part of the CFs will be oxidized to produce defects, resulting in a decrease in the RCF mechanical properties.³⁴ In comparison with VCFs, the tensile strength of RCFs was maintained at above 73% and the RCFs obtained under the condition of P500T15D550T30 maintained the highest tensile strength (about 99.42% of that of VCFs). Hao et al.³⁵ studied the effect of different pyrolysis temperatures on the tensile properties of RCFs. Under the condition of oxidation at 550 °C for 30 min, the tensile strength loss was 13–20%. Figure 4b shows the tensile modulus of RCFs. With an increase in oxidation temperature and oxidation time, the tensile modulus increased continuously. In comparison with VCFs, the tensile modulus of RCFs remains about 87.21% at the lowest level and increases to 118.69% of that of VCFs at the highest level. Zabihi et al.³⁶ reported that the tensile modulus of CFs recycled by a microwave-assisted chemical method was slightly improved by about 1.7%. The high retention rate of tensile strength and tensile modulus indicates that microwave pyrolysis can recycle high-quality CFs.

In Figure 4c, the recovery rates of RCFs were calculated according to the weight of CFs recycled under various reaction conditions. Under the condition of P400T15D500T40, the highest recovery rate (97.9%) was obtained. Under the condition of P500T15D550T40, the lowest recovery rate

(96.4%) was obtained. With the increase in reaction temperature and time, the recovery rate of RCFs decreased gradually. However, the recovery rate of RCFs can exceed 96% under all conditions. The recovery loss is caused by the decomposition of the sizing agent on CF surface and the partial oxidation of CFs; thus, an increase in temperature will also reduce the recovery rate.

3.3. Structural Changes of RCFs. XRD, Raman, FT-IR, and XPS were used to study the changes of the carbon structure, composition, and free radicals of RCFs. To analyze the structural changes of RCFs, XRD patterns under different conditions are shown in Figure 5a. The calculation and analysis results of Figure 5a are given in Table 2. The diffraction peaks of all (002) crystal planes shift to the left, which means that the unit cell parameters become larger and the crystal plane spacing becomes larger. In comparison with VCFs, the half-peak width of the diffraction peak of RCFs on the (002) crystal plane becomes larger, while the grain size of the (101) crystal plane becomes smaller, which means that the crystallinity is reduced, resulting in the formation of defects and damage to the microstructure of RCFs. These may lead to the degradation of the mechanical properties of RCFs.

As shown in Figure 5b, two Raman peaks of CFs can be observed at around 1360 and 1580 cm^{-1} . The D peak at 1360 cm^{-1} represents the defect and graphitization disorder degree of carbon atoms, and the G peak at 1580 cm^{-1} represents the in-plane stretching vibration of sp^2 hybridization of C atoms. The intensity ratio R (I_D/I_G) reflects the disorder degree of carbon atoms. The smaller the R value, the higher the crystal integrity of CFs and the higher the proportion of ordered structure of carbon atoms.⁶ With an increase in reaction temperature and reaction time, the Raman shift of the D peak decreases and the R value increases, indicating the decrease of the graphitization degree of RCFs. Jeong et al.³⁴ considered that a decrease in R value could increase the tensile strength of

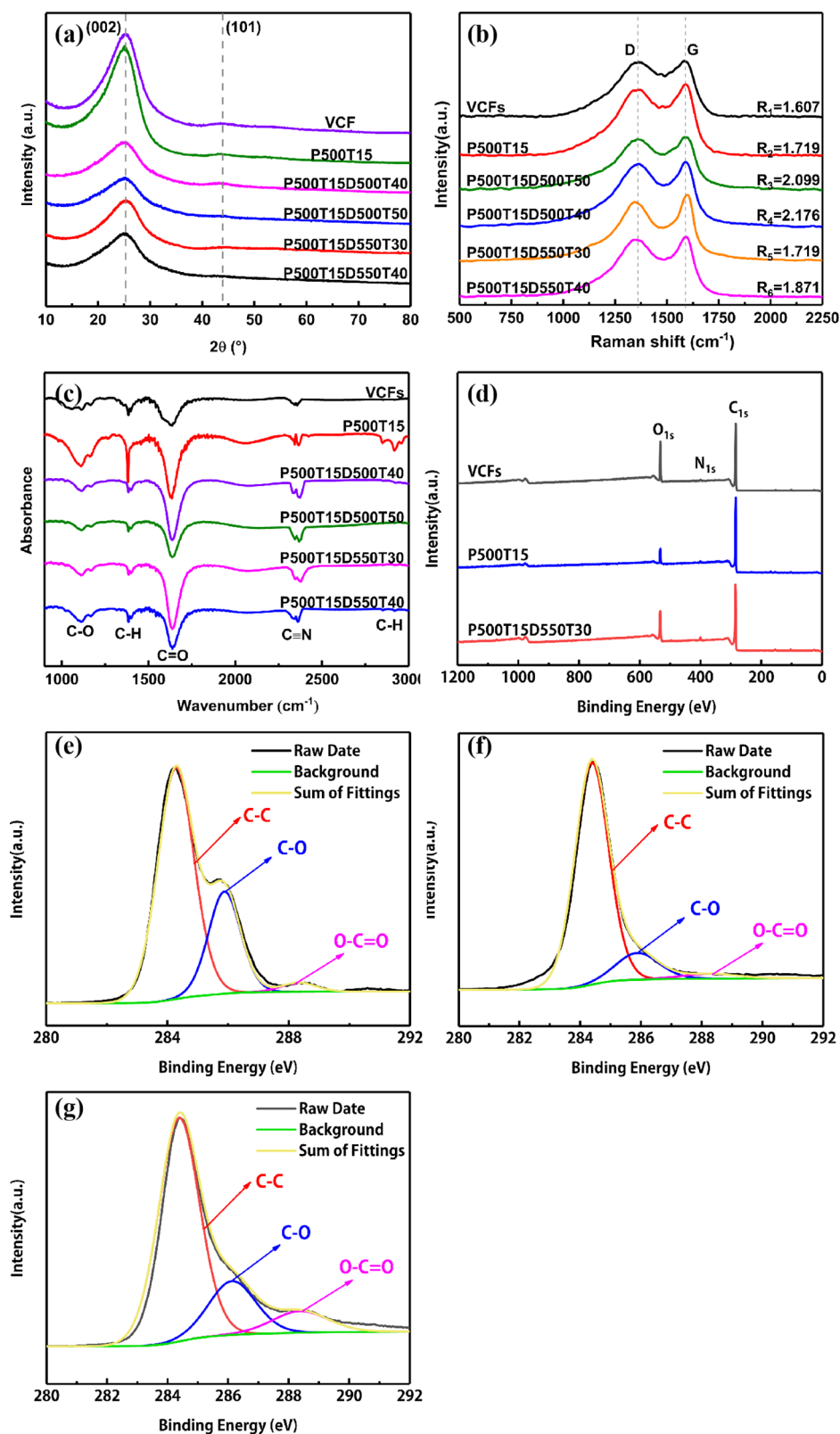


Figure 5. XRD patterns (a), Raman (b), FT-IR (c), and total XPS spectra (d) of RCFs and C_{1s} spectra of VCFs (e), P500T15 (f), and P500T15D550T30 (g).

RCFs. According to the results of this study, the change in tensile strength with the R value is consistent with the previous report.

The FT-IR spectra of RCFs are shown in Figure 5c. The tensile vibration peaks of the methyl C–H bonds at 2960 and

2920 cm^{-1} , the bending vibration peaks of the methyl group at 1380 cm^{-1} , and the tensile vibration peaks of the methylene group at 2850 cm^{-1} are all observed. The peaks at 2370 and 2340 cm^{-1} are caused by the tensile vibration of the $\text{C}\equiv\text{N}$ bond, and the peak at 1630 cm^{-1} corresponds to the tensile

Table 2. Lattice Parameters of RCFs^a

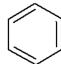
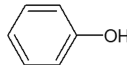
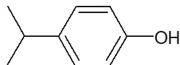
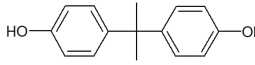
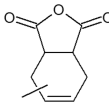
	(002) peak			L_c (Å)	(101) peak			L_a (Å)
	2θ (deg)	d_{002} (Å)	fwhm (deg)		2θ (deg)	d_{101} (Å)	fwhm (deg)	
VCFs	25.04	3.63	5.33	15.11	43.71	2.56	2.98	28.43
P500T15	24.86	3.67	5.51	14.64	43.83	2.59	3.22	26.41
D500T40	24.80	3.69	5.27	15.27	43.74	2.59	3.15	26.88
D500T50	24.78	3.70	5.39	14.95	43.72	2.61	3.10	27.38
D550T30	24.86	3.64	5.44	14.79	43.64	2.58	3.11	27.37
D550T40	24.86	3.67	5.37	14.95	43.64	2.55	3.16	26.87

^a 2θ is the position of the diffraction peak, fwhm is the half-peak width of the diffraction peak, d_{002} and d_{101} are the longitudinal and transverse plane spacings of the crystal in RCFs, L_c is the thickness of the (002) plane, and L_a is the grain size of the (101) plane.

Table 3. Contents of Elements and Functional Groups in RCFs

	element content (%)			functional group content (%)			
	C	O	N	O/C	C–C	C–O	O–C=O
VCFs	80.35	17.79	1.86	22.14	69.85	27.50	2.64
P500T15	86.85	10.03	3.12	11.55	84.15	12.81	3.04
D550T30	78.41	18.36	3.22	23.42	74.33	22.31	3.36

Table 4. Compositions of Pyrolytic Gases and Pyrolytic Oils

Gases	Chemical formula	Peak area (%)	Oils	Chemical formula	Peak area (%)
Carbon monoxide	CO	52.87	Benzene		37.61
Methane	CH ₄	14.66	Phenol		23.31
Carbon dioxide	CO ₂	24.10	P-isopropyl phenol		6.83
Ethylene	C ₂ H ₄	4.45	Bisphenol A		21.84
Ethane	C ₂ H ₆	3.92	Methyl tetrahydrophthalic anhydride		10.41

vibration of the C=O bond. The symmetrical tensile vibrations of the C–O bond are located at 2960 and 2920 cm⁻¹. In comparison with VCFs, the peaks of methyl and methylene groups and the C–O bond of the residual solid P500T15 are increased significantly, which was caused by the organic matter attached to the surface of CFs after pyrolysis. After an oxidation treatment of the residual solid, the intensity of the methyl peak at 1380 cm⁻¹ and the C–O bond peak at 1110 cm⁻¹ decreased, and the methyl peaks at 2960 and 2920 cm⁻¹ and the methylene peak at 2850 cm⁻¹ disappeared, which was similar to the case for VCFs, indicating that the oxidation treatment had a good recycling effect and could achieve the

expected purpose. Kim et al.¹⁸ observed similar functional groups in their study and found that these functional groups could form covalent interfacial bonds with –COOH groups in the cross-linked polymer adhesives, effectively transfer the stress between the matrix and fibers, and improve the interfacial adhesion.

XPS was used to further study the chemical structure of the surface of RCFs, as shown in Figure 5d–g. For VCFs and RCFs, the spectra contain three main peaks, which represent carbon (C 1s, 284.99 eV), nitrogen (N 1s, 400.17 eV), and oxygen (O 1s, 532.42 eV), respectively. Table 3 shows the contents of elements and functional groups in the CFs. In

comparison with VCFs, the content of N atoms in RCFs increased, which was due to the incomplete removal of sizing agents according to a study by Liu et al.³⁷ This can also be seen in the FT-IR spectra in Figure 5c, where the intensity of the C≡N peak of RCFs is stronger than that of VCFs. The differences between the functional groups on VCFs and RCFs were further studied by fitting C 1s spectra, and the percentages of functional groups are shown in Table 3. As shown in Figure 5e–g, the main peaks of C 1s spectra include C–C (284.43 eV), C–O (286.28 eV), and O–C=O (288.63 eV), where C–O and O–C=O correspond to the functional groups C–OH and –COOH, respectively.

As shown in Table 3, in comparison with VCFs, the lower O/C ratio during CFRP pyrolysis results in higher contents of C and N atoms and C–C bonds but lower contents of O atoms and C–O bonds. After the pyrolysis of epoxy resin, C and N atoms remained on the surface of CFs, while O atoms were released. After the oxidation of the residual solids, the contents of C atoms and C–C bonds decreased, while the contents of O atoms, C=O bonds and C–O bonds increased, leading to a higher O/C ratio. Therefore, it can be inferred that the oxidation of carbon leads to the breakage of C–C and C=C bonds, resulting in the formation of C=O and C–O bonds.³⁶ The proportion of functional groups of RCFs regenerated after oxidation treatment is similar to that of VCFs, indicating that the regeneration effect of CFs is significant.

3.4. Composition Analysis of Pyrolysis Products. To study the composition of the resin matrix after pyrolysis, GC-MS was used to analyze the composition of the pyrolysis products at 500 °C. As shown in Table 4, the gas products mainly include carbon monoxide, carbon dioxide, methane, ethane, and ethylene and the liquid products mainly include benzene, phenol, *p*-isopropylphenol, bisphenol A, and methyl tetrahydrophthalic anhydride. Bisphenol A is the monomer of the epoxy resin, which is separated from the cured epoxy resin, and further decomposes into benzene, phenol and *p*-isopropylphenol. This provides a reference for the harmless treatment of pyrolysis products.

4. CONCLUSION

In this work, CFs were successfully recycled from CFRPs by microwave pyrolysis combined with an oxidation process. The resin matrix in CFRP was rapidly decomposed by microwave pyrolysis. The pyrolytic carbon and organic residues on the surface of CFs were removed by oxidation at 500–550 °C for 30–50 min, and finally RCFs with a smooth surface were obtained. The RCFs retained good mechanical properties. The tensile strength ranged from 2243.81 to 3042.90 MPa, and the tensile modulus ranged from 195.40 to 265.94 GPa. After microwave pyrolysis and oxidation treatment, the chemical bond types of CFs did not change significantly. For the resin decomposition product, the main components were carbon monoxide, carbon dioxide, methane, ethane, and ethylene in the gaseous product and the major liquid components were benzene, phenol, *p*-isopropylphenol, bisphenol A, and methyl tetrahydrophthalic anhydride. In short, RCFs with excellent properties can be obtained from CFRPs by microwave pyrolysis combined with an oxidation process. It has a huge market potential and is has promise to be scaled up in the future.

AUTHOR INFORMATION

Corresponding Authors

Lei Xu – Faculty of Metallurgical and Energy Engineering, Kunming University of Science and Technology, Kunming 650093, People's Republic of China; State Key Laboratory of Complex Nonferrous Metal Resources Clean Utilization and Key Laboratory of Unconventional Metallurgy, Ministry of Education, Kunming University of Science and Technology, Kunming 650093, People's Republic of China; orcid.org/0000-0001-7130-8625; Email: xu_lei@kust.edu.cn

Zhigang Shen – Sinopec Shanghai Research Institute of Petrochemical Technology, Shanghai 201208, People's Republic of China; Email: shenzg.sshy@sinopec.com

Authors

Yiyao Ren – Faculty of Metallurgical and Energy Engineering, Kunming University of Science and Technology, Kunming 650093, People's Republic of China

Xiaobiao Shang – Key Laboratory of Unconventional Metallurgy, Ministry of Education, Kunming University of Science and Technology, Kunming 650093, People's Republic of China

Rongzheng Fu – Sinopec Shanghai Research Institute of Petrochemical Technology, Shanghai 201208, People's Republic of China

Wei Li – Key Laboratory of Unconventional Metallurgy, Ministry of Education, Kunming University of Science and Technology, Kunming 650093, People's Republic of China

Lirong Guo – Faculty of Metallurgical and Energy Engineering, Kunming University of Science and Technology, Kunming 650093, People's Republic of China

Complete contact information is available at:

<https://pubs.acs.org/10.1021/acsomega.1c06652>

Author Contributions

Y.R.: methodology, data curation, investigation, writing-original draft. L.X.: conceptualization, supervision, writing-review and editing, formal analysis, visualization, validation. X.S.: software, formal analysis. Z.S.: investigation, testing. R.F.: investigation, testing. W.L.: writing-review and editing, validation. L.G.: methodology, data curation.

Notes

The authors declare no competing financial interest.

ACKNOWLEDGMENTS

This work was financially supported by the National Natural Science Foundation of China (Grant No. 51864030), the China Petrochemical Corporation (No. 219037), the National Key R&D Program of China (Nos. 2018YFC1901904), the Yunnan Basic Research Key Project (Nos. 202101AS070023), the Yunnan Provincial Science and Technology Talents Program (No. 2019HB003), the Yunnan Science and Technology Major Project (Grant Nos. 2019ZE001), and the Yunnan Provincial youth top-notch talent support program.

REFERENCES

- (1) Verma, S.; Balasubramaniam, B.; Gupta, R. K. Recycling, reclamation and re-manufacturing of carbon fibres. *Curr. Opin. Green. Sust.* **2018**, *13*, 86–90.
- (2) Giorgini, L.; Benelli, T.; Brancolini, G.; Mazzocchetti, L. Recycling of carbon fiber reinforced composites waste to close their

- life cycle in a cradle-to-cradle approach. *Curr. Opin. Green. Sust.* **2020**, *26*, 100368.
- (3) Bae, J. S.; Bae, J. H.; Woo, H. J.; Lee, B. J.; Jeong, E. G. Novel thermoplastic toughening agents in epoxy matrix for vacuum infusion process manufactured composites. *Carbon. Lett.* **2018**, *25*, 43–49.
- (4) Pellegrini-Cervantes, M. J.; Barrios-Durstewitz, C. P.; Núñez-Jaquez, R. E.; Baldenebro-Lopez, F. J.; Corralal-Higuera, R.; Arredondo-Rea, S. P.; Rodriguez-Rodriguez, M.; Llanes-Cardenas, O.; Beltran-Chacon, R. Performance of carbon fiber added to anodes of conductive cement-graphite pastes used in electrochemical chloride extraction in concretes. *Carbon. Lett.* **2018**, *26*, 18–24.
- (5) Abdou, T. R.; Botelho, A. B., Jr.; Espinosa, D. C. R.; Tenório, J. A. S. Recycling of polymeric composites from industrial waste by pyrolysis: deep evaluation for carbon fibers reuse. *Waste. Manage.* **2021**, *120*, 1–9.
- (6) Pakdel, E.; Kashi, S.; Varley, R.; Wang, X. Recent progress in recycling carbon fibre reinforced composites and dry carbon fibre wastes. *Resour. Conserv. Recy.* **2021**, *166*, 105340.
- (7) Zhang, J.; Chevali, V. S.; Wang, H.; Wang, C. H. Current status of carbon fibre and carbon fibre composites recycling. *Compos. Part. B-Eng.* **2020**, *193*, 108053.
- (8) Okajima, I.; Sako, T. Recycling of carbon fiber-reinforced plastic using supercritical and subcritical fluids. *J. Mater. Cycles. Waste.* **2017**, *19*, 15–20.
- (9) Dang, W.; Kubouchi, M.; Sembokuya, H.; Tsuda, K. Chemical recycling of glass fiber reinforced epoxy resin cured with amine using nitric. *Polymer.* **2005**, *46*, 1905–1912.
- (10) Nahil, M. A.; Williams, P. T. Recycling of carbon fibre reinforced polymeric waste for the production of activated carbon fibres. *J. Anal. Appl. Pyrol.* **2011**, *91*, 67–75.
- (11) Yip, H. L. H.; Pickering, S. J.; Rudd, C. D. Characterisation of carbon fibres recycled from scrap composites using fluidised bed process. *Plast. Eubber. Compos.* **2002**, *31*, 278–282.
- (12) Matrenichev, V. V.; Clara, M.; Belone, L.; Palola, S.; Sarlin, E. Resizing approach to increase the viability of recycled fibre-reinforced composites. *Materials.* **2020**, *13*, 5773.
- (13) Palmer, J.; Ghita, O. R.; Savage, L.; Evans, K. E. Successful closed-loop recycling of thermoset composites. *Compos. Part. A-App. S.* **2009**, *40*, 490–498.
- (14) Yildirim, E.; Onwudili, J. A.; Williams, P. T. Recovery of carbon fibres and production of high quality fuel gas from the chemical recycling of carbon fibre reinforced plastic wastes. *J. Supercrit. Fluid.* **2014**, *92*, 107–114.
- (15) Lester, E.; Kingman, S.; Wong, K. H.; Rudd, C.; Pickering, S.; Hilal, N. Microwave heating as a means for carbon fibre recovery from polymer composites: a technical feasibility study. *Mater. Res. Bull.* **2004**, *39*, 1549–1556.
- (16) Henry, L.; Schneller, A.; Doerfler, J.; Mueller, W. M.; Aymonier, C.; Horn, S. Semi-continuous flow recycling method for carbon fibre reinforced thermoset polymers by near- and supercritical solvolysis. *Polym. Degrad. Stab.* **2016**, *133*, 264–274.
- (17) Knappich, F.; Klotz, M.; Schlummer, M.; Wlling, J.; Murer, A. Recycling process for carbon fiber reinforced plastics with polyamide 6, polyurethane and epoxy matrix by gentle solvent treatment. *Waste. Manage.* **2019**, *85*, 73–81.
- (18) Kim, Y. N.; Kim, Y. O.; Kim, S. Y.; Park, M.; Yang, B.; Kim, J.; Jung, Y. C. Application of supercritical water for green recycling of epoxy-based carbon fiber reinforced plastic. *Compos. Sci. Technol.* **2019**, *173*, 66–72.
- (19) Yang, J.; Liu, J.; Liu, W.; Wang, J.; Tang, T. Recycling of carbon fibre reinforced epoxy resin composites under various oxygen concentrations in nitrogen-oxygen atmosphere. *J. Anal. Appl. Pyrol.* **2015**, *112*, 253–261.
- (20) Jiang, G.; Pickering, S. J.; Walker, G. S.; Wong, K. H.; Rudd, C. D. Surface characterisation of carbon fibre recycled using fluidised bed. *Appl. Surf. Sci.* **2008**, *254*, 2588–2593.
- (21) Kim, K. W.; Lee, H. M.; An, J. H.; Chung, D. C.; An, K. H.; Kim, B. J. Recycling and characterization of carbon fibers from carbon fiber reinforced epoxy matrix composites by a novel super-heated-steam method. *J. Environ. Manage.* **2017**, *203*, 872.
- (22) Boulanghien, M.; R'Mili, M.; Bernhart, G.; Berthet, F.; Soudais, Y. Mechanical characterization of carbon fibres recycled by steam thermolysis. *Adv. Mater. Sci. Eng.* **2018**, *2018*, 1–10.
- (23) Meng, F.; Mckechnie, J.; Turner, T.; Wong, K. H.; Pickering, S. J. Environmental Aspects of Use of Recycled Carbon Fiber Composites in Automotive Applications. *Environ. Sci. Technol.* **2017**, *51*, 12727–12736.
- (24) Meng, F.; Elsa, O.; Zhao, Y.; Chang, J. C.; Pickering, S. J.; Jon, M. Comparing Life Cycle Energy and Global Warming Potential of Carbon Fiber Composite Recycling Technologies and Waste-Management Options. *ACS. Sustain. Chem. Eng.* **2018**, *6*, 9854–9865.
- (25) Pimenta, S.; Pinho, S. T. Recycling carbon fibre reinforced polymers for structural applications: technology review and market outlook. *Waste. Manage.* **2011**, *31*, 378–392.
- (26) Deng, J.; Xu, L.; Zhang, L.; Peng, J.; Koppala, S. Recycling of carbon fibers from cfrp waste by microwave thermolysis. *Processes.* **2019**, *7*, 207.
- (27) Sabzevari, B.; Koleini, S. J.; Ghassa, S.; Shahbazi, B.; Chelgani, S. C. Microwave-leaching of copper smelting dust for Cu and Zn extraction. *Materials.* **2019**, *12*, 1822.
- (28) Pindar, S.; Dhawan, N. Evaluation of in-situ microwave reduction for metal recovery from spent lithium-ion batteries. *Sustain. Mater. Techno.* **2020**, *25*, No. e00201.
- (29) Zhu, Z.; Xu, L.; Han, Z.; Liu, J.; Zhang, L.; Yang, C.; Xu, Z.; Liu, P. Defluorination study of spent carbon cathode by microwave high-temperature roasting. *J. Environ. Manage.* **2022**, *302*, 114028.
- (30) Kwon, K. H.; Chen, X. J.; Min, K. S.; Yun, Z. Recycling of sewage sludge using microwave pretreatment and elutriated acid fermentation. *Desalin. Water. Treat.* **2015**, *53*, 2363–2368.
- (31) Sun, J.; Wang, W.; Liu, Z.; Ma, C. Recycling of waste printed circuit boards by microwave-induced pyrolysis and featured mechanical processing. *Ind. Eng. Chem. Res.* **2011**, *50*, 11763–11769.
- (32) Lester, E.; Kingman, S.; Wong, K. H.; Rudd, C.; Pickering, S.; Hilal, N. Microwave heating as a means for carbon fibre recovery from polymer composites: a technical feasibility study. *Mater. Res. Bull.* **2004**, *39*, 1549–1556.
- (33) Mazzocchetti, L.; Benelli, T.; D'Angelo, E.; Leonardi, C.; Zattini, G.; Giorgini, L. Validation of carbon fibers recycling by pyro-gasification: the influence of oxidation conditions to obtain clean fibers and promote fiber/matrix adhesion in epoxy composites. *Compos. Part. A-App. S.* **2018**, *112*, 504–514.
- (34) Jeong, J. S.; Kim, K. W.; An, K. H.; Kim, B. J. Fast recovery process of carbon fibers from waste carbon fibers-reinforced thermoset plastics. *J. Environ. Manage.* **2019**, *247*, 816–821.
- (35) Hao, S.; He, L.; Liu, J.; Liu, Y.; Liu, X. Recovery of Carbon Fiber from Waste Prepreg via Microwave Pyrolysis. *Polymers. Basel.* **2021**, *13*, 1231.
- (36) Zabihi, O.; Ahmadi, M.; Liu, C.; Mahmoodi, R.; Li, Q.; Naebe, M. Development of a low cost and green microwave assisted approach towards the circular carbon fibre composites. *Compos. Part. B-Eng.* **2020**, *184*, 107750.
- (37) Liu, W.; Huang, H.; Cheng, H.; Liu, Z. CFRP reclamation and remanufacturing based on a closed-loop recycling process for carbon fibers using supercritical n-butanol. *Fiber. Polym.* **2020**, *21*, 604–618.